Nuclear Engineering and Technology 51 (2019) 818–824

Contents lists available at ScienceDirect

Nuclear Engineering and Technology

journal homepage: www.elsevier.com/locate/net

Original Article

Evaluation of gamma-ray and neutron attenuation properties of some polymers

M.R. Kaçal [a, *], F. Akman [b], M.I. Sayyed [c], F. Akman [d]

[a] Giresun University, Arts and Sciences Faculty, Department of Physics, 28100, Giresun, Turkey
[b] Bingöl University, Vocational School of Technical Sciences, Department of Electronic Communication Technology, 12000, Bingöl, Turkey
[c] University of Tabuk, Faculty of Science, Department of Physics, Tabuk, Saudi Arabia
[d] Bingöl University, Vocational School of Technical Sciences, 12000, Bingöl, Turkey

ARTICLE INFO

Article history:
Received 6 November 2018
Received in revised form
19 November 2018
Accepted 20 November 2018
Available online 21 November 2018

Keywords:
Polymer
Neutron
Gamma photon
Attenuation
Shielding

ABSTRACT

In the present work, we determined the gamma-ray attenuation characteristics of eight different polymers(Polyamide (Nylon 6) (PA-6), polyacrylonitrile (PAN), polyvinylidenechloride (PVDC), polyaniline (PANI), polyethyleneterephthalate (PET), polyphenylenesulfide (PPS), polypyrrole (PPy) and polytetrafluoroethylene (PTFE)) using transmission geometry utilizing the high resolution HPGe detector and different radioactive sources in the energy range 81–1333 keV. The experimental linear attenuation coefficient values are compared with theoretical data (WinXCOM data). The linear attenuation coefficient of all polymers reduced quickly with the increase in energy, at the beginning, while decrease more slowly in the region from 267 keV to 835 keV. The effective atomic number of PVDC and PTFE are comparatively higher than the Z_{eff} of the remaining polymers, while PA-6 possesses the lowest effective atomic number. The half value layer results showed that PTFE (C_2F_4, highest density) is more effective to attenuate the gamma photons. Also, the theoretical results of macroscopic effective removal cross section for fast neutrons ($\sum_R$) were computed to investigate the neutron attenuation characteristics. It is found that the $\sum_R$ values of the eight investigated polymers are close and ranged from 0.07058 cm^{-1} for PVDC to 0.11510 cm^{-1} for PA-6.

1. Introduction

Nowadays, nuclear technology is frequently used in a wide range such as material identification, agriculture, medical applications, nuclear power plants, scientific and space exploration. Many novel shielding materials have been developed and studied by the researchers [1–8] to protect humans from the ionizing radiation generated by radioactive sources. In general, the gamma-ray and neutron attenuation coefficients characterize the radiations interaction with a material. As is well known, materials which contain elements with high atomic number (such as Ba, Pb and Bi) are used to attenuate gamma-rays, while materials which contain elements with low atomic number are preferred in attenuating neutron particles. However, the accurate values of the radiation attenuation parameters of materials containing elements with low atomic number such as C, H, O and N are very important in some medical applications. In medical applications, materials containing low atomic number elements such as polymers and plastics are often used as tissue equivalent and phantom materials. In this context, it is very important to investigate the parameters such as mass attenuation coefficients (μ/ρ), linear attenuation coefficient (μ), half-value layer (HVL), tenth value layer (TVL), effective atomic number (Z_{eff}), and exposure buildup factor (EBF), which are the indicator of the interaction of polymers with gamma-rays. Furthermore, the polymers are one of the materials which can be preferred as a neutron attenuation material. Water which contains high amount of hydrogen elements is generally used for neutron attenuation. However, water is liquid at room temperature and this may be its disadvantage in some applications. Since the materials such as polymers and plastics containing high amount of hydrogen elements are solid at room temperature, it is a good alternative to replace water for neutron shielding. A number of studies have been reported in the literature regarding the interaction of polymers with gamma-rays and/or neutrons [9–20].

Polymers also play a very important role in facilitating human-life. Even, the human body contains polymers such as proteins, enzymes. Polymers are widely used in everyday life such as electronics, medical applications, drug delivery system, cosmetics,

* Corresponding author.
E-mail address: mustafa.kacal@giresun.edu.tr (M.R. Kaçal).

https://doi.org/10.1016/j.net.2018.11.011

tissue engineering, etc. In this study, Polyamide (Nylon 6) (PA-6), polyacrylonitrile (PAN), polyvinylidenechloride (PVDC), polyaniline (PANI), polyethyleneterephthalate (PET), polyphenylenesulfide (PPS), polypyrrole (PPy) and polytetrafluoroethylene (PTFE) were selected as polymer samples. PA-6 is a polymer having very low dielectric constant, excellent mechanical performance, chemical resistance and high melting temperature [21]. PAN is a polymer used in applied areas such as textiles and electronics since it has an excellent thermal stability, high electrolyte up-take and a leading material for the production of carbon fibers [22,23]. PVDC is one of the most preferred polymers in heavy ion irradiation studies [24]. Besides, PANI and PPy, which are conductive polymers, are used in many application fields. PANI is generally used in energy storage applications, while PPy has an excellent charge-storage capability [25,26]. Rechargeable PANI batteries and high capacity PPy capacitors are products used in the field of electronics. PET is a material use in biotechnology, medicine and tissue engineering. In addition, it has a wide range of applications in microelectronics areas [27]. On the other hand, PPS and PTFE possess high thermal and chemical stability and they are used actively in many applications in the industry [28,29]. These excellent properties make polymers important in the production of various materials for nuclear industry. Since these polymers are frequently used in industry and in daily-life, the knowledge of their interaction with radiation will contribute to applied sciences.

The aim of this study was to determine the gamma-ray and neutron attenuation characteristics of the selected polymers. The experimental and theoretical results of μ, HVL, TVL, MFP and Z_{eff}, and theoretical results of EBF were determined to investigate the gamma-ray attenuation characteristics. Also, the theoretical results of macroscopic effective removal cross section for fast neutrons were computed to investigate the neutron attenuation characteristics. The experiments were executed in transmission geometry utilizing the high resolution HPGe detector and different radioactive sources in the energy range 81–1333 keV.

2. Theoretical background

The gamma-ray attenuation characteristics of the shielding material can be tested by calculating different parameters such as μ, HVL, TVL, MFP, Z_{eff} and EBF. Linear attenuation coefficient, which is defined as the probability per unit path length that a photon will interact with the absorber, is a significant parameter in the characterization of the gamma radiation in a material. This parameter differs according to the incident photon energy, the mass density and atomic number of the material. The linear attenuation coefficient can be determined using Beer-Lambert's law with the following equation:

$$I = I_0 e^{-\mu x} \tag{1}$$

where, I_0 and I are the intensities of the primary (emitted from the radioactive source) and passing through the absorber, μ is the linear attenuation coefficient and x is the absorber thickness.

Many radiation attenuation parameters such as μ/ρ, HVL, TVL, MFP and Z_{eff} can be determined by using the linear attenuation coefficient. The μ/ρ can be obtained mathematically by dividing the linear attenuation coefficient to mass density of the absorber. The required absorber thickness which reduces the initial radiation intensity to 50% after passing through the absorber is called half value layer and it is obtained using the following equation [30]:

$$HVL = \frac{0.693}{\mu} \tag{2}$$

The required absorber thickness which lowers the initial radiation intensity to 10% after passing through the absorber is known as tenth value layer and it determines using Eq. (3) [31]:

$$TVL = \frac{2.303}{\mu} \tag{3}$$

The required absorber thickness which reduces the initial radiation intensity to 36.8% after passing through the absorber is called mean free path and it derives using Eq. (4) [32]:

$$MFP = {}^{1}/_{\mu} \tag{4}$$

If a material has low HVL, TVL and MFP values, this indicates that this material is a good shielding material.

Another useful parameter in selecting an alternative to a material used in radiation shielding is the effective atomic number. Because the effective atomic number depends on the photon energy, it is not the right way to identify it with a single number. The effective atomic number, which is related to photon energy, can be obtained by Eq. (5) [33]:

$$Z_{eff} = \frac{\sum_i f_i A_i (\mu/\rho)_i}{\sum_j f_j \frac{A_j}{Z_j} (\mu/\rho)_j} \tag{5}$$

where f_i implies the ratio of ith element number to total element number in the material, A_i and Z_i indicate the atomic weight and atomic number of ith element in the material.

The determination of buildup factors is very important for correcting the energy storage in different shielding materials. When the photon penetrates into the substance, its energy decreases and the dose buildup occurs in the material. Dose storage in the material depends on the intensity of the photon. The gamma-ray buildup factor is a multiplicative factor that is used to obtain the correction factor for un collided photons containing the contribution of scattered photons. It can be defined as the ratio of the total detector response to the un collided photons. For the present polymer samples, we used the G-P fitting method to calculate the EBF. This method is described in details elsewhere [17].

On the other hand, for the present polymers, the values of the macroscopic removal cross-section ($\sum_R$) can be calculated by the next equation [7]:

$$\sum_R = \sum_i W_i \left(\sum_R / \rho \right)_i \tag{6}$$

where$(\sum_R/\rho)_i$ (cm^2/g) is the mass removal cross-section of the ith constituent.

3. Experimental process

In the present work, the incident (Io) and the transmitted (I) gamma rays intensities for PA-6, PAN, PVDC, PANI, PET, PPS, PPy and PTF polymers were measured at photons energies emitted by ^{22}Na (511 and 1275 keV), ^{54}Mn (835 keV), ^{57}Co (122 and 136 keV), ^{60}Co (1173 and 1332 keV), ^{133}Ba (81, 161, 276, 303, 356 and 384 keV), and ^{137}Cs (662 keV) radioactive point sources. The measurements were carried out using the HPGe detector(GEM-SP7025P4-B model) connected with high voltage source 2600 V with positive polarity, multichannel analyzer (DSPEC-JR 2.0 V.046 model), absorber polymer samples, collimators in a geometrical set-up and a radioactive point source as shown given in Fig. 1. The detector window-sample and sample-source distances were set to 28 cm and 35 cm, respectively. Furthermore, the I and Io gamma ray intensities were repeated three times to minimize the statistical error at each

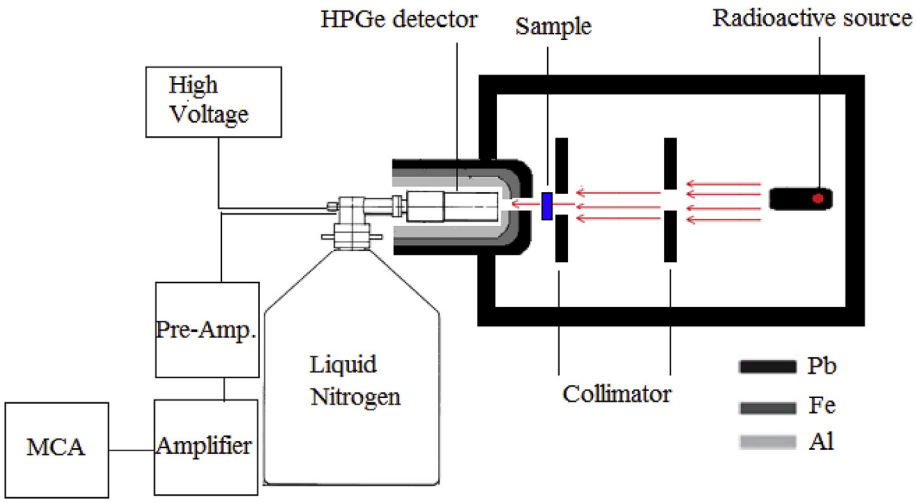

Fig. 1. Experimental setup.

energy value. Experimental explanations for the present measurements have been given with details in previous studies [1–3].

4. Results and discussion

The linear attenuation coefficients (μ) for the present polymers (given in Table 1) were measured under narrow beam condition. The measurements were carried out at 14 photon energies from 81 keV to 1333 keV (as discussed in the previous section). The experimental results of μ for the selected polymer samples are listed in Table 2. For experimental verification of the μ, the WinXCOM [34] results for the present samples were also presented in Table 2. As indicates from Table 2, the experimental μ values are very close to the theoretical WinXCOM data. The difference between experimental and WinXCOM μ is in the range of 0.60–5.86%, 0.14–5.40%, 0.78–4.05%, 0.22–4.08%, 1.02–4.20%, 0.96–4.04%, 0.38–3.53% and 0.42–4.36% for PA-6, PAN, PVDC, PANI, PET, PPS, PPy and PTFE, respectively. The experimental μ results for the eight polymers were plotted in Fig. 2. The results of μ are in line with the work carried out by Vahabi et al. [19] who used the MCNP5 code to investigate the attenuation parameters for some polymers such as Poly-propylene, Perspex, Teflon, Bakelite, and Nylon 6-6 between 59.5 keV and 1332.5 keV. Also, the variation in μ with the energy shown in Fig. 2 is in accordance with that found in the literature for polycarbonate, polyvinyl alcohol, Polytetrafluoroethylene, Polyethylene terephthalate and Polymethyl methacrylate [16].

As seen in Fig. 2, the μ of all polymers fall quickly with the increase in energy, at the beginning, due to the fast decrease with energy of the photoelectric absorption coefficient. The curves decrease more slowly in the region from 267 keV to 835 keV where Compton Effect is more important [1]. From Fig. 2, it is clear that below 303 keV the difference between the μ of the polymers is comparatively wider and decreases progressively as the energy of photon increases. At low energies, the μ depends on both the atomic number and the mass density of the sample and hence the difference between the attenuation coefficients is relatively larger. For example, for PA-6 and PPS, the difference in the experimental μ at 81 keV is 0.056, while this difference in μ between the two samples at 303 keV reduces to 0.015. But at high energies, the μ is independent of the atomic number and all polymers absorb nearly the same amount of radiation. For instance, the difference between μfor PA-6 and PTFE at 1333 keV is only 0.006. From Fig. 2, it is seen that the μ values of PTFE (C_2F_4) are comparatively higher than those of other polymers. These high values may be due to higher density of this polymer than others. This indicates that PTFE shows much higher radiation absorption characteristics than the rest of polymers under study.

The effective atomic number (Z_{eff}) of the present polymers was calculated from the determined mass attenuation coefficients. The obtained results are exhibited graphically in Fig. 3. From Fig. 3, it is obvious that the Z_{eff} of PVDC and PTFE are comparatively higher than the Z_{eff} of the remaining polymers. This higher value is mainly due to Chlorine (Cl) content in PVDC, and since the hydrogen content is negligible in PTFE and it contains fluorine (F). Also, Fig. 3 shows that the Z_{eff} of PAN (C_3H_3N) and PANI (C_6H_4NH) are almost the same but comparatively lower than PA-6. The Z_{eff} values for PA-6 ($C_6H_{11}NO$) are the lowest among the polymers under study since it contains comparatively the highest percentage of hydrogen. It is evident from Fig. 3 that the Z_{eff} values remain almost constant for all polymers. This trend in Z_{eff} of the eight polymers is due to the fact that these polymers composed of elements of much close atomic numbers (mainly H, C, N, and O). The same trend in Z_{eff} for

Table 1
Abbreviation, chemical formula and the density of the selected polymers.

Sample	Abbreviation	Chemical formula	Density (gcm^{-3})
Polyamide (Nylon 6)	PA-6	$C_6H_{11}NO$	1.13
Polyacrylonitrile	PAN	C_3H_3N	1.18
Polyvinylidenechloride	PVDC	$C_2H_2Cl_2$	1.63
Polyaniline	PANI	C_6H_4NH	1.36
Polyethyleneterephthalate	PET	$C_{10}H_8O_4$	1.38
Polyphenylenesulfide	PPS	C_6H_4S	1.35
Polypyrrole	PPy	C_4H_3N	1.48
Polytetrafluoroethylene	PTFE	C_2F_4	2.20

Table 2
Linear attenuation coefficients (cm^{-1}) using WinXCOM and experimental for the selected polymers.

Energy (keV)	PA-6		PAN		PVDC		PANI	
	Exp.	Theo.	Exp.	Theo.	Exp.	Theo.	Exp.	Theo.
81	0.2025 ± 0.0073	0.1991	0.1952 ± 0.0076	0.2001	0.3847 ± 0.0179	0.3911	0.2322 ± 0.0062	0.2299
122	0.1749 ± 0.0069	0.1774	0.1854 ± 0.0079	0.1784	0.2663 ± 0.0061	0.2711	0.2018 ± 0.0079	0.2051
136	0.1627 ± 0.0039	0.1717	0.1644 ± 0.0067	0.1727	0.2605 ± 0.0068	0.2529	0.2007 ± 0.0093	0.1986
161	0.1539 ± 0.0019	0.1635	0.1668 ± 0.0027	0.1644	0.2405 ± 0.0048	0.2315	0.1912 ± 0.0061	0.1891
276	0.1304 ± 0.0029	0.1362	0.1368 ± 0.0048	0.1370	0.1871 ± 0.0066	0.1819	0.1536 ± 0.0065	0.1576
303	0.1326 ± 0.0039	0.1317	0.1392 ± 0.0064	0.1325	0.1804 ± 0.0056	0.1751	0.1566 ± 0.0037	0.1524
356	0.1246 ± 0.0037	0.1239	0.1178 ± 0.0053	0.1246	0.1585 ± 0.0040	0.1638	0.1447 ± 0.0054	0.1433
384	0.1230 ± 0.0062	0.1203	0.1245 ± 0.0033	0.1209	0.1613 ± 0.0062	0.1587	0.1366 ± 0.0045	0.1392
511	0.1096 ± 0.0035	0.1070	0.1043 ± 0.0047	0.1076	0.1416 ± 0.0062	0.1405	0.1241 ± 0.0042	0.1238
662	0.0976 ± 0.0029	0.0956	0.1003 ± 0.0039	0.0962	0.1202 ± 0.0056	0.1253	0.1135 ± 0.0033	0.1107
835	0.0881 ± 0.0026	0.0860	0.0825 ± 0.0035	0.0864	0.1096 ± 0.0020	0.1124	0.1013 ± 0.0025	0.0995
1173	0.0704 ± 0.0018	0.0729	0.0750 ± 0.0033	0.0733	0.0983 ± 0.0027	0.0951	0.0871 ± 0.0015	0.0843
1275	0.0675 ± 0.0018	0.0698	0.0721 ± 0.0029	0.0702	0.0945 ± 0.0035	0.0912	0.0816 ± 0.0017	0.0808
Energy (keV)	PET		PPS		PPy		PTFE	
	Exp.	Theo.	Exp.	Theo.	Exp.	Theo.	Exp.	Theo.
1333	0.0664 ± 0.0020	0.0682	0.0720 ± 0.0022	0.0686	0.0878 ± 0.0034	0.0892	0.0757 ± 0.0013	0.0789
81	0.2284 ± 0.0040	0.2330	0.2586 ± 0.0099	0.2617	0.2465 ± 0.0092	0.2485	0.3711 ± 0.0059	0.3573
122	0.2030 ± 0.0038	0.2065	0.2155 ± 0.0088	0.2115	0.2181 ± 0.0085	0.2215	0.3130 ± 0.0058	0.3084
136	0.1949 ± 0.0026	0.1997	0.2058 ± 0.0078	0.2020	0.2220 ± 0.0049	0.2145	0.2960 ± 0.0048	0.2972
161	0.1927 ± 0.0021	0.1900	0.1860 ± 0.0036	0.1898	0.2048 ± 0.0102	0.2042	0.2706 ± 0.0039	0.2817
276	0.1608 ± 0.0022	0.1581	0.1609 ± 0.0068	0.1550	0.1650 ± 0.0082	0.1701	0.2418 ± 0.0036	0.2330
303	0.1510 ± 0.0023	0.1528	0.1482 ± 0.0064	0.1497	0.1596 ± 0.0083	0.1645	0.2225 ± 0.0039	0.2252
356	0.1373 ± 0.0021	0.1437	0.1444 ± 0.0062	0.1405	0.1577 ± 0.0058	0.1547	0.2037 ± 0.0034	0.2117
384	0.1366 ± 0.0032	0.1395	0.1324 ± 0.0047	0.1363	0.1529 ± 0.0055	0.1502	0.2081 ± 0.0052	0.2055
511	0.1294 ± 0.0021	0.1242	0.1260 ± 0.0053	0.1211	0.1364 ± 0.0042	0.1337	0.1879 ± 0.0031	0.1827
662	0.1098 ± 0.0019	0.1109	0.1061 ± 0.0043	0.1081	0.1235 ± 0.0032	0.1195	0.1609 ± 0.0027	0.1632
835	0.1034 ± 0.0021	0.0997	0.0946 ± 0.0040	0.0971	0.1092 ± 0.0036	0.1073	0.1434 ± 0.0033	0.1467
1173	0.0860 ± 0.0014	0.0845	0.0847 ± 0.0035	0.0823	0.0903 ± 0.0023	0.0910	0.1189 ± 0.0020	0.1243
1275	0.0835 ± 0.0014	0.0810	0.0793 ± 0.0028	0.0789	0.0894 ± 0.0021	0.0872	0.1139 ± 0.0022	0.1191
1333	0.0766 ± 0.0013	0.0791	0.0747 ± 0.0027	0.0771	0.0855 ± 0.0029	0.0852	0.1186 ± 0.0021	0.1164

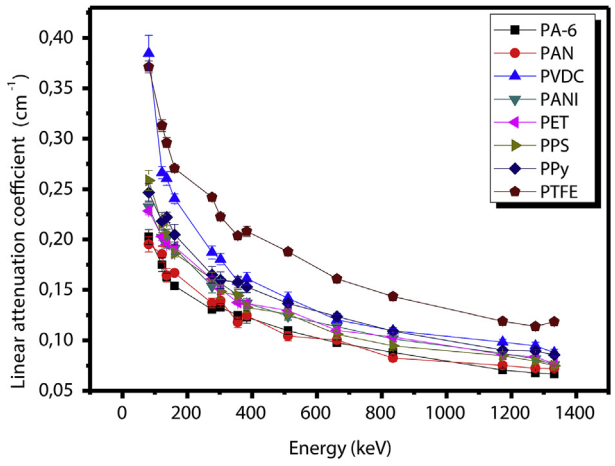

Fig. 2. The experimental linear attenuation coefficients (cm^{-1}) for the selected polymers.

some alloys such as steel, bronze and brass was reported by El-Kateb et al. [35].

The HVL is frequently used in the calculations of photon penetration in shielding materials. HVL is the minimum thickness of a sample at which the transmitted gamma radiation intensity is half of that of the original intensity. The calculated HVL for the present polymers are given in Fig. 4 (a), which shows an increasing trend of HVL values for the all polymers with the increasing in the energy from 81 keV to 1333 keV. The increase in HVL indicates more photons are likely to be penetrated. It is known that the higher HVL leads to worsen in the shielding of incoming photons, therefore, for practical applications, the samples with lower HVL are more effective in reducing gamma photons. Fig. 4 (a) revealed that the HVL of PTFE (C_2F_4) is less than the remaining polymers which shows that this polymer is more effective to attenuate the gamma photons. Since PTFE has a greater density than the other selected polymer samples, its HVL values are smaller than the other samples. HVL is higher for PA-6 ($C_6H_{11}NO$) and PAN (C_3H_3N), this means these two polymers have worse attenuation ability among the selected polymers.

The variation of TVL and MFP with the energy for the selected polymers is exhibited in Fig. 4(b and c). Apparently, the trend of variation in both TVL and MFP for all polymers with the energy is comparable to the variation noticed by HVL (Fig. 4-a), however the difference is in the magnitude. PTFE (C_2F_4, highest density) has the lowest MFP as well as TVL, which confirms the effectiveness of this polymer to attenuate more gamma photons.

The calculated Z_{eq} values for the present polymers were shown in Table S3, while the G-P fitting parameters for PA-6 (as an example) are listed in Table S4. EBF of given polymers variation with photon energy between 0.015 and 15 MeV were illustrated in graphical form at fixed penetration depth values (Fig. 5a–d). The similar trend was observed for other polymers reported in the literature [36].

Obviously, the EBF results presented in the figure show an increasing trend with the increment of energy up to moderate energy zone. Besides, at 10 and 40 mfp in the moderate region of energy, the EBF values look very large which is owing to the Compton scattering process, where the photons are not totally removed but their energies were reduced. The presence of these photons is found for a long time in the sample, which results in multiple Compton scattering, and this rise the EBF to maximum values between 0.08 and 0.5 MeV [37]. The EBF values for all

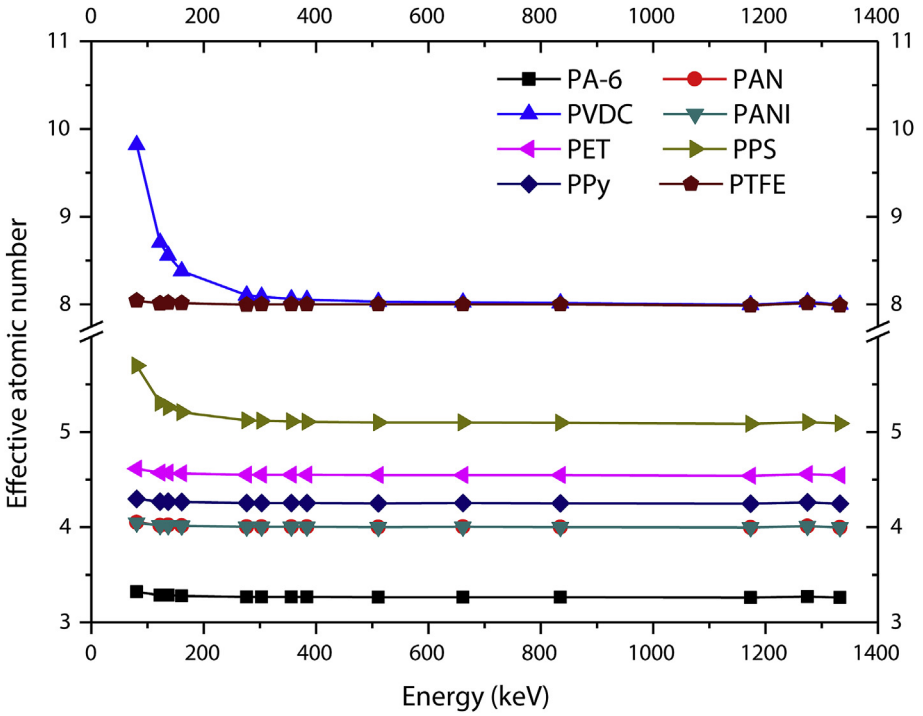

Fig. 3. The variation of the effective atomic number with the energy for the selected polymers.

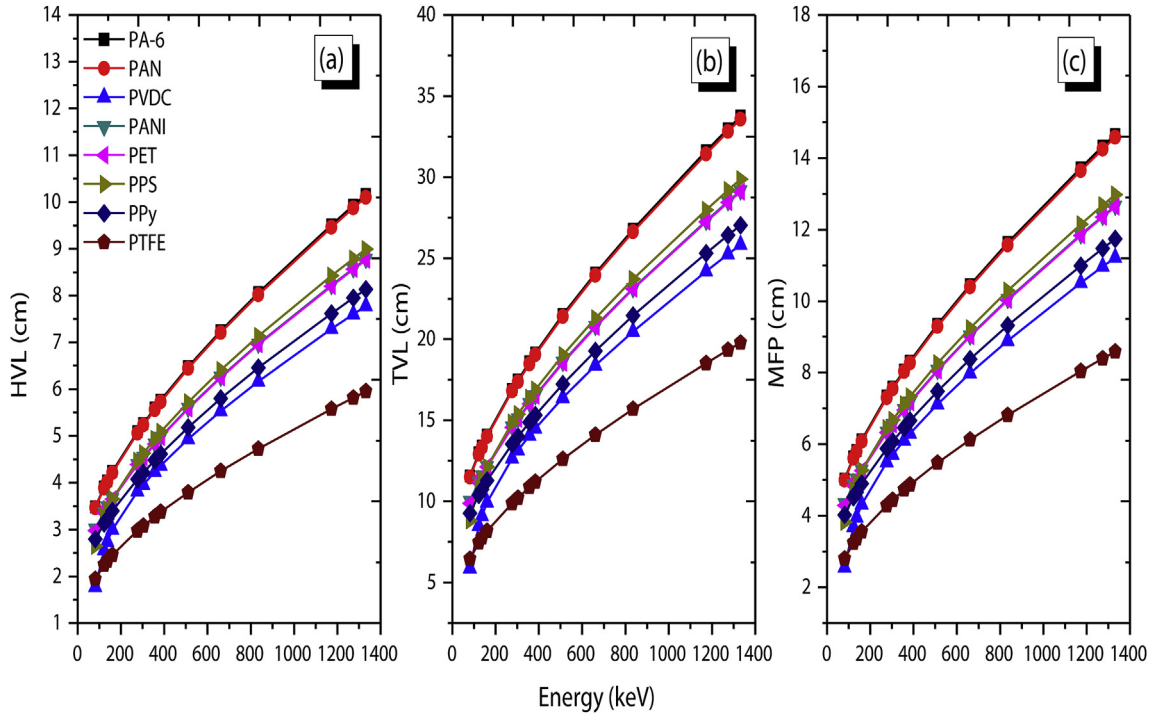

Fig. 4. The variation of the (a) half value layer (b) tenth value layer and (c) mean free path with the energy for the selected polymers.

polymer samples under study nearly show same values between 3 and 15 MeV, which indicates that the EBF is independent of the composition of the polymers in this energy region. The trend in EBF between 3 and 15 MeV is owing to that the pair production which is the most important process at these high energies [38]. Moreover, PANI has the highest EBF values among the selected polymers. Also, PVDC and PPS have the lowest EBF values. The low EBF values for both PVDC and PPS can be attributed to the high Z_{eq} for these two polymers (PVDC contains chlorine, while PPS contains sulphur and these two elements rise the Z_{eq} for these two samples).

Also, it was found from Fig. 5a–d that the EBF values of the polymers increase with the penetration depths. Lowest values for EBF for all samples are found at 1 mfp (Fig. 5-a), while the highest EBF values are observed at 40 mfp (Fig. 5-d). This can be ascribed to

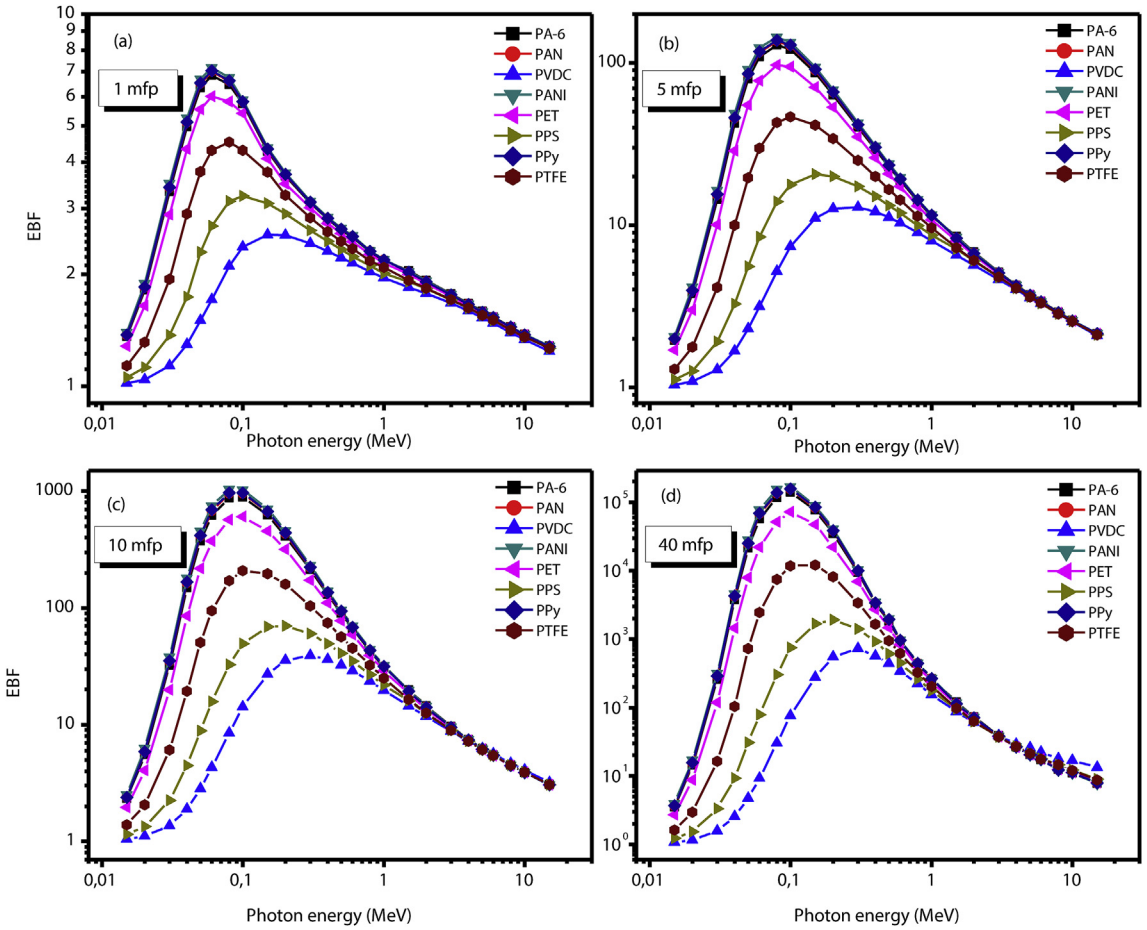

Fig. 5. The variation of the exposure buildup factor with the energy for the selected polymers.

multiple scattering for large penetration depths. On other words, the increase in penetration depth leads to increase the interaction of the photons with the sample which results in generation of large number of low energy photons. This is in line with the previous studies reported by Sayyed et al. [39] who reported the EBF for some smart polymers such as Poly vinyliden fluoride, Dimethyl sulfoxide, Polyethersulfone and Polyvinylidene chloride.

The $\sum_R$ for the polymers under study was calculated and the results are plotted in Fig. 6. It is obvious from Fig. 6 that the $\sum_R$ values of the eight investigated polymers are close and ranged from 0.07058 cm^{-1} for PVDC (density = 1.63 g cm^{-3}) to 0.1151 cm^{-1} for PA-6(density = 1.13 g cm^{-3}). This is due to the fact that most the polymer samples contain mainly hydrogen and carbon with differences in their weight fractions. It is well known that the light elements (such as hydrogen) is one of the most important parameter that affecting the neutron attenuation for any material. Therefore, from Table 1 we can see that PA-6 contains the largest number of hydrogen atoms, hence this sample contains the highest weight fraction of hydrogen and this explains the high $\sum_R$ value of PA-6, while the lowest weight fraction in the polymers (If we excluded PTFE) is found in PVDC, and this explains the low $\sum_R$ value of this polymer. However, PTFE does not contain hydrogen, but its $\sum_R$ is higher than some polymers such as PPS and PVDC. This can be explained according the high density of this polymer. Therefore, we can say that the density of the polymer also can affect the neutron attenuation. The $\sum_R$ values of all polymers (except PVDC, PPS and PTFE) are higher than the $\sum_R$ value of ordinary concrete reported by Bashter [40]. Also, the $\sum_R$ of the present polymers are slightly smaller than those reported of Polyethylenimine [15] and resin 250WD [41].

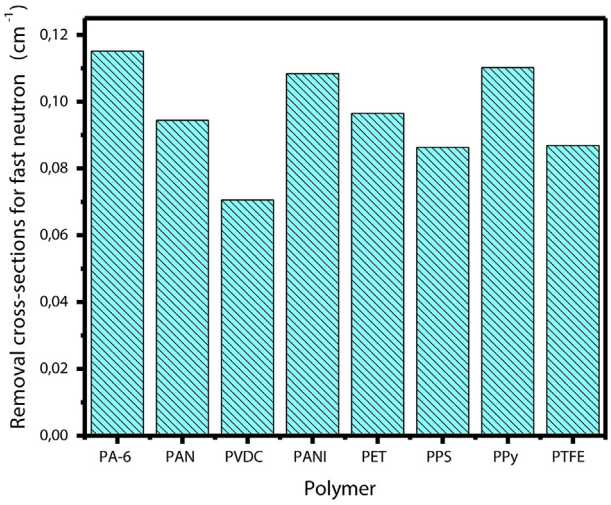

Fig. 6. The removal cross section for fast neutron for the selected polymers.

5. Conclusions

The gamma-ray and neutron attenuation properties of some selected polymers such as PA-6, PAN, PVDC, PANI, PET, PPS, PPy and

PTFE were investigated. The neutron attenuation properties were investigated using the macroscopic effective removal cross section for fast neutrons parameter. The gamma-ray attenuation characteristics were investigated utilizing the μ, HVL, TVL, MFP, Z_{eff} and EBF parameters. The experimental process was carried out using transmission geometry at 14 photon energies from 81 keV to 1333 keV. The maximum μ values were determined for PVDC sample. The Z_{eff} values of PVDC and PTFE are comparatively higher than the Z_{eff} values of the remaining polymers. Also, the HVL, TVL and MFP results of PTFE are less than the remaining polymers which shows that this polymer is more effective to attenuate the gamma-rays. It is observed that the EBF values of PANI were seen tend to be high among to chosen polymers. The EBF values of the selected polymers increase with the penetration depths and they were lowest for 1 mfp and highest for 40 mfp. While the maximum Σ_R value was observed for PA-6, the minimum Σ_R value was obtained for PVDC. In addition, the Σ_R values of selected polymers generally higher than the Σ_R value of ordinary concrete in neutron shielding. Moreover, the gamma-ray attenuation parameters are particularly useful in the field of medical applications such as tissue equivalent and phantom materials.

Acknowledgements

The present work was done with the support of the Scientific Research Projects Coordination Unit of Giresun University under Project no: FEN-BAP-A-160317-23.

Appendix A. Supplementary data

Supplementary data to this article can be found online at https://doi.org/10.1016/j.net.2018.11.011.

References

[1] F. Akman, M.I. Sayyed, M.R. Kaçal, H.O. Tekin, Investigation of photon shielding performances of some selected alloys by experimental data, theoretical and MCNPX code in the energy range of 81 keV-1333 keV, J. Alloy. Comp. 772 (2019) 516–524.
[2] M.I. Sayyed, F. Akman, I.H. Geçibesler, H.O. Tekin, Measurement of mass attenuation coefficients, effective atomic numbers, and electron densities for different parts of medicinal aromatic plants in low-energy region, Nucl. Sci. Tech. 29 (2018) 144.
[3] F. Akman, I.H. Geçibesler, M.I. Sayyed, S.A. Tijani, A.R. Tufekci, I. Demirtas, Determination of some useful radiation interaction parameters for waste foods, Nuclear Engineering and Technology 50 (6) (2018) 944–949.
[4] M.I. Sayyed, Bismuth modified shielding properties of zinc boro-tellurite glasses, J. Alloy. Comp. 688 (2016) 111–117.
[5] R. El-Mallawany, M.I. Sayyed, M.G. Dong, Comparative shielding properties of some tellurite glasses: Part 2, J. Non-Cryst. Solids 474 (2017) 16–23.
[6] H.O. Tekin, T. Manici, Simulations of mass attenuation coefficients for shielding materials using the MCNP-X code, Nucl. Sci. Tech. 28 (2017) 95.
[7] G. Lakshminarayana, S.O. Baki, K.M. Kaky, M.I. Sayyed, H.O. Tekin, A. Lira, I.V. Kityk, M.A. Mahdi, Investigation of structural, thermal properties and shielding parameters for multicomponent borate glasses for gamma and neutron radiation shielding applications, J. Non-Cryst. Solids 471 (2017) 222–237.
[8] S.A.M. Issa, M.I. Sayyed, M.H.M. Zaid, K.A. Matari, Photon parameters for gamma-rays sensing properties of some oxide of lanthanides, Results in Physics 9 (2018) 206–210.
[9] C.V. More, R.R. Bhosale, P.P. Pawar, Detection of new polymer materials as gamma-ray-shielding materials, Radiat. Eff. Defect Solid 175 (5–6) (2017) 469–484.
[10] M. Büyükyıldız, M.A. Taşdelen, Y. Karabul, M. Çağlar, O. İçelli, E. Boydaş, Measurement of photon interaction parameters of high-performance polymers and their composites, Radiat. Eff. Defect Solid 173 (5–6) (2018) 474–488.
[11] N. Kucuk, M. Cakir, N.A. Isitman, Mass attenuation coefficients, effective atomic numbers and effective electron densities for some polymers, Radiat. Protect. Dosim. 153 (1) (2013) 127–134.
[12] V.P. Singh, N.M. Badiger, N. Kucuk, Assessment of methods for estimation of effective atomic numbers of common human organ and tissue substitutes: waxes, plastics and polymers, Radioprotection 49 (2) (2014) 115–121.
[13] O. Gurler, U.A. Tarım, Determination of radiation shielding properties of some polymer and plastic materials against gamma-rays, ActaPhysicaPolonica A 130 (2016) 236–238.
[14] R.R. Bhosale, C.V. More, D.K. Gaikwad, P.P. Pawar, M.N. Rode, Radiation shielding and gamma ray attenuation properties of some polymers, Nucl. Technol. Radiat. Protect. 32 (3) (2017) 288–293.
[15] M.I. Sayyed, Investigation of shielding parameters for smart polymers, Chin. J. Phys. 54 (2016) 408–415.
[16] R. Mirji, B. Lobo, Computation of the mass attenuation coefficient of polymeric materials at specific gamma photon energies, Radiaiton Physics and Chemistry 135 (2017) 32–44.
[17] H.C. Manjunatha, A study of gamma attenuation parameters in poly methyl methacrylate and Kapton, Radiat. Phys. Chem. 137 (2017) 254–259.
[18] K.S. Mann, A. Rani, M.S. Heer, Shielding behaviors of some polymer and plastic materials for gamma-rays, Radiat. Phys. Chem. 106 (2015) 247–254.
[19] S.M. Vahabi, M. Bahreinipour, M.S. Zafarghandi, Determining the mass attenuation coefficients for some polymers using MCNP code: a comparison study, Vacuum 136 (2017) 73–76.
[20] V.P. Singh, S.P. Shirmardi, M.E. Medhat, N.M. Badiger, Determination of mass attenuation coefficient for some polymers using Monte Carlo simulation, Vacuum 119 (2015) 284–288.
[21] T. Vedamurthy, M. Murugesan, Synthesis, characterization, and evaluation of the hydrophobic, dielectric properties of phenols functionalized nylon 6 polymers by zinc acetate catalyst using Mannich reaction, Mater. Chem. Phys. 216 (2018) 517–525.
[22] X. Shi, J. Jiang. Anionic polymerization initiated by lithium amides for preparing high molecular weight polyacrynitrile. Chin. Chem. Lett., https://doi.org/10.1016/j.celet.2018.01.040.
[23] C. He, J. Liu, J. Li, F. Zhu, H. Zhao, Blending based polyacrynitrile/poly(vinyl alcohol) membrane for rechargeable lithium ion batteries, J. Membr. Sci. 560 (2018) 30–37.
[24] K.S. Samra, S. Thakur, L. Singh, Photoluminescent and thermal behavior of 120 MeV silicon and 84 MeV oxygen ion irradiated PVDC, J. Lumin. 131 (2011) 686–694.
[25] A. Eftekhari, L. Li, Y. Yang, Polyanilinesupercapasitors. Journal of Power Sources 347 (2017) 86–107.
[26] Y. Meng, L. Zhang, R. Xing, H. Huang, Y. Qu, T. Jiao, J. Zhou, Q. Peng, Facile preportion and electrochemical characterization of self-assembled core-shell diamond-polypyrrolenanocomposites, Colloids Surf., A 55 (2018) 787–794.
[27] A. Reznickova, Z. Kolska, K. Zaruba, V. Svorcik, Grafting of gold nanoparticles on polyethylenetere phthalate using dithiol interlayer, Mater. Chem. Phys. 145 (2014) 484–490.
[28] T. Hisamatsu, S. Nakano, T. Adachi, M. Ishikawa, K. Iwakura, The effect of compatibility on toughness of PPS/SEBS polymer alloy, Polymer 41 (2000) 4803–4809.
[29] Y. Wu, C. Sun, Y. Wu, Y. Xing, J. Xiao, B. Guo, Y. Wang, Y. Sui, The degradation behavior and mechanism of polytetrafluoroethylene under low energy proton irradiation, Nucl. Instrum. Methods Phys. Res. B 430 (2018) 47–53.
[30] M.I. Sayyed, F. Akman, V. Turan, A. Araz. Evaluation of radiation absorption capacity of some soil samples.Radiochim. Acta, https://doi.org/10.1515/ract-2018-2996.
[31] M.R. Kacal, F. Akman, M.I. Sayyed. Investigation of radiation shielding properties for some ceramics.Radiochim. Acta, https://doi.org/10.1515/ract-2018-3030.
[32] B.O. Elbashir, M.G. Dong, M.I. Sayyed, S.A.M. Issa, K.A. Matori, M.H.M. Zaid, Comparison of Monte Carlo simulation of gamma ray attenuation coefficients of amino acids with XCOM program and experimental data, Results in Physics 9 (2018) 6–11.
[33] F. Akman, R. Durak, M.R. Kacal, F. Bezgin, Study of absorption parameters around the K edge for selected compounds of Gd, X Ray Spectrom. 45 (2016) 103–110.
[34] L. Gerward, N. Guilbert, K.B. Jensen, H. Levring, WinXCOM- a program for calculating X-ray attenuation coefficients, Radiat. Phys. Chem. 71 (2004) 653–654.
[35] A.H. El-Kateb, R.A.M. Rizk, A.M. Abdul-Kader, Determination of atomic cross-sections and effective atomic numbers for some alloys, Ann. Nucl. Energy 27 (2000) 1333–1343.
[36] T. Singh, N. Kumar, P.S. Singh, Chemical composition dependence of exposure buildup factors for some polymers, Ann. Nucl. Energy 36 (2009) 114–120.
[37] P.S. Singh, T. Singh, P. Kaur, Variation of energy absorption buildup factors with incident photon energy and penetration depth for some commonly used solvents, Ann. Nucl. Energy 35 (2008) 1093–1097.
[38] M.I. Sayyed, G. Lakshminarayana, I.V. Kityk, M.A. Mahdi, Evaluation of shielding parameters for heavy metal fluoride based tellurite-rich glasses for gamma ray shielding applications, Radiat. Phys. Chem. 139 (2017) 33–39.
[39] M.I. Sayyed, M.Y. AlZaatreh, K.A. Matori, H.A.A. Sidek, M.H.M. Zaid, Comprehensive study on estimation of gamma-ray exposure buildup factors for smart polymers as a potent application in nuclear industries, Results in Physics 9 (2018) 585–592.
[40] I.I. Bashter, Calculation of radiation attenuation coefficients for shielding concretes, Ann. Nucl. Energy 24 (1997) 1389–1401.
[41] Y. Elmahroug, B. Tellili, C. Souga, Determination of shielding parameters for different types of resins, Ann. Nucl. Energy 63 (2014) 619–623.